ELSEVIER

Ligand assisted homolytic cleavage of the Ru–Ru single bond in [Ru$_2$(CO)$_4$]$^{2+}$ core and the chemical consequence

Sanjib K. Patra, Moumita Majumdar, Jitendra K. Bera *

Department of Chemistry, Indian Institute of Technology, Kanpur 208016, India

Abstract

The Ru–Ru single bond in [Ru$_2$(CO)$_4$(MeCN)$_6$][BF$_4$]$_2$ remains intact in the reaction with 2-*i*-propyl-1,8-naphthyridine (*i*PrNP) and the isolated product is the *cis*-[Ru$_2$(*i*PrNP)$_2$(CO)$_4$(OTf)$_2$] (1) obtained via crystallization in the presence of [*n*-Bu$_4$N][OTf]. The 2-*t*-butyl-1,8-naphthyridine (*t*BuNP), on the contrary, leads to the oxidative cleavage of the Ru–Ru single bond resulting in the *trans*-[Ru(*t*BuNP)$_2$(MeCN)$_2$][BF$_4$]$_2$[NC(Me)C(Me)N] (2). The *anti*-[NC(Me)C(Me)N]$^{2-}$ is the product of the two-electron reductive coupling of two acetonitrile molecules. The phenoxo appendage in 2-(2-hydroxyphenyl)-1,8-naphthyridine (hpNP) brings the identical effect of the scission of the Ru–Ru bond but the process is non-oxidative and the product obtained is the *cis*-[Ru(hpNP)$_2$(CO)$_2$][BF$_4$] (3). The bis-(diphenylphosphino)methane (dppm) in dichloromethane oxidatively cleave the Ru–Ru bond leading to chloro bridged [Ru-(μ-Cl)(dppm)(CO)(MeCN)]$_2$[BF$_4$]$_2$ (4). All the complexes have been characterized by the spectroscopic and electrochemical measurements and their structures have been established by X-ray diffraction study.
© 2006 Elsevier B.V. All rights reserved.

Keywords: Metal–metal bond; Ruthenium; 1,8-Naphthyridine; Reductive coupling; Homolytic cleavage

1. Introduction

The utility of the 1,8-naphthyridine (NP) based ligands to engage dimetal units has been demonstrated in the literature [1]. We have been involved in the metal–metal bonded dimetal chemistry that employs the tridentate ligand L3 comprised of a NP core and a donor unit attached covalently at 2-position. One typical example is 2-(2-thiazolyl)-1,8-naphthyridine (tzNP) that binds the diruthenium unit as shown in Scheme 1. Ligands with furyl, thiazolyl and pyridyl appendages have been shown to form *cis*-[Ru$_2$(CO)$_4$(L3)$_2$]$^{2+}$ [2].

The present work stems from further exploration on the NP based ligands those introduce sterically demanding groups at sites *trans* to Ru–Ru single bond in [Ru$_2$]$^{2+}$ complexes. We report here the reaction of [Ru$_2$(CO)$_4$-(CH$_3$CN)$_6$][BF$_4$]$_2$ with the ligands 2-*i*-propyl-1,8-naphthyri-dine (*i*PrNP), 2-*t*-butyl-1,8-naphthyridine (*t*BuNP), 2-(2-hydroxyphenyl)-1,8-naphthyridine (hpNP) and bis-(diphenylphosphino)methane (dppm) depicted in Scheme 2. The roles of different appendages in the NP based ligands are probed in causing the scission of the Ru–Ru single bond. The rupture of the Ru–Ru bond assisted by the bulky dppm ligands is also reported. Homolytic cleavage of the Ru–Ru single bond produce the Ru based radical species and the chemical reactions that ensue are discussed.

2. Results and discussion

2.1. Ligand assisted cleavage of the Ru–Ru single bond

The reaction of *i*PrNP with [Ru$_2$(CO)$_4$(MeCN)$_6$][BF$_4$]$_2$ and subsequent crystallization in the presence of [*n*-Bu$_4$N]-[OTf] provide the diruthenium complex *cis*-[Ru$_2$(*i*PrNP)$_2$-(CO)$_4$(OTf)$_2$] (1) (Scheme 3a). The use of *t*BuNP, however, leads to the cleavage of the Ru–Ru single bond yielding the mononuclear complex *trans*-[Ru(*t*BuNP)$_2$(MeCN)$_2$][BF$_4$]$_2$-[NC(Me)C(Me)N] (2) (Scheme 3b). The 2-hydroxyphenyl

* Corresponding author. Tel.: +91 512 2597336; fax: +91 512 2597436.
  E-mail address: jbera@iitk.ac.in (J.K. Bera).
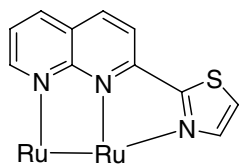
Scheme 1.
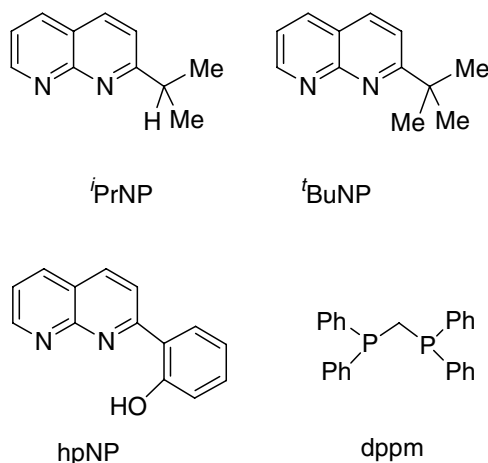
Scheme 2.

attachment to NP causes the similar scission of the Ru–Ru single bond and produce cis-[Ru(hpNP)$_2$(CO)$_2$][BF$_4$] (3) (Scheme 3c). The chloro bridged dimeric complex [Ru-(μ-Cl)(dppm)(CO)(MeCN)]$_2$[BF$_4$]$_2$(4) is isolated from the reaction of [Ru$_2$(CO)$_4$(MeCN)$_6$][BF$_4$]$_2$ with dppm (Scheme 3d).

The NP based ligands with furyl, thiazolyl or pyridyl attachments at 2-position form diruthenium complexes cis-[Ru$_2$(CO)$_4$(L3)$_2$]$^{2+}$ [2]. The 2-methyl-1,8-naphthyridine (MeNP) reacts readily with [Ru$_2$(CO)$_4$(MeCN)$_6$][OTf]$_2$ to form cis-[Ru$_2$(MeNP)$_2$(CO)$_4$(OTf)$_2$] and the molecular structure of the product has been established in our laboratory [3]. The bulk of the appendages in the NP ligands are increased gradually and the products are analyzed. The i-propyl group in 2-i-propyl-1,8-naphthyridine (^{i}PrNP) produces the cis-[Ru$_2$(^{i}PrNP)$_2$(CO)$_4$(OTf)$_2$] (1) in which the Ru–Ru single bond remains intact. Further increase in the size of the appendage to t-butyl in 2-t-butyl-1,8-naphthyridine leads to the oxidative cleavage of the Ru–Ru sin-

gle bond resulting in the trans-[Ru(^{t}BuNP)$_2$(MeCN)$_2$]-[BF$_4$]$_2$[NC(Me)C(Me)N] (2). The highest yield of 2 is achieved in acetonitrile as reaction solvent although an identical product was recovered in dichloromethane but in low yield. The plausible cause of the Ru–Ru bond cleavage is the size of the t-butyl group attachment to the NP. A preliminary molecular modeling investigation reveals substantial steric crowding between the hydrogens of the t-butyl group and the Ru atom in the hypothetical '[Ru$_2$-(^{t}BuNP)$_2$(CO)$_4$]' constructed by substituting the Me group by t-butyl in '[Ru$_2$(MeNP)$_2$(CO)$_4$]' [3]. The finding of this work illustrates the size limit of the axial groups in the scission of the metal–metal bond.

The spectroscopic and electrochemical behavior of the complex 1 is reminiscent of other [Ru$_2$(CO)$_4$]$^{2+}$ complexes containing NP ligands [2,3]. The ^{1}H NMR spectroscopy of 1 displays five resonances in the aromatic region corresponding to five aromatic protons of the ^{i}PrNP. A two proton isopropyl methyne signal for two ligands appears at δ 4.35 ppm and the six proton methyl resonances of each of the ligands appear separately at δ 1.71 ppm and δ 1.47 ppm. The cyclic voltammogram of complex 1 exhibits an irreversible metal based oxidation at $E_{p,a}$ = +1.29 V and the reduction profile involves four irreversible waves centered at −0.87, −1.07, −1.34 and −1.59 V.

Careful analyses of 2 reveal that the metal–metal bond cleavage reaction is accompanied by oxidation of the Ru^I in the precursor molecule to Ru^{IV} in trans-[Ru(^{t}BuNP)$_2$-(MeCN)$_2$]$^{4+}$ unit. It should be noted here that the oxidative scission of the Ru–Ru bond occurs even under strict dry and anaerobic condition throughout the reaction and crystallization process. The loss of CO in the final product is the consequence of the high oxidation state of the metal ion. The anti-[NC(Me)C(Me)N]$^{2-}$ dianion was assigned from the X-ray structure of the molecule. It is believed that the source of the dianion is the two-electron reductive coupling of the acetonitrile molecules (vide infra).

Complex 2 is essentially diamagnetic. The ^{1}H NMR spectroscopy of complex 2 displays five resonances in the aromatic region corresponding to five aromatic protons of ^{t}BuNP, indicating the equivalence of two ligands on the NMR time scale. It displays a singlet at 1.70 ppm for the protons of t-butyl groups of ^{t}BuNP. The signals for the coordinated MeCN appear at δ 2.20 ppm. The
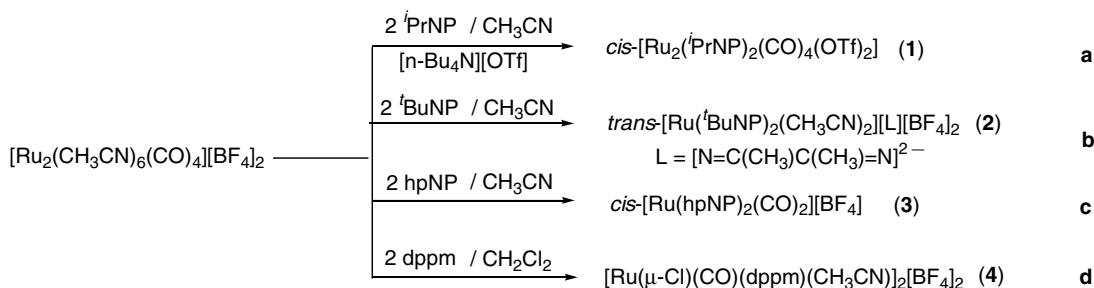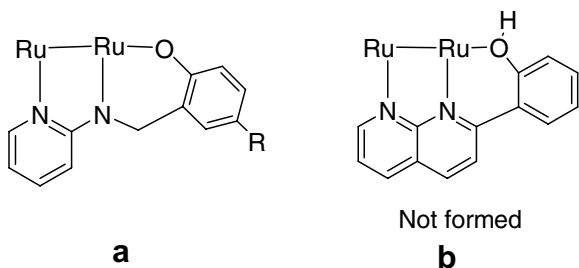

Scheme 3.

methyl protons of the *anti*-[NC(Me)C(Me)N]$^{2-}$ dianion appear at δ 2.07 ppm as singlet. Complex **2** exhibits a broad irreversible oxidation at $E_{p,a} = +1.64$ V assigned as Ru^{IV}/Ru^V couple. The ligand based reduction occurs at $E_{p,c} = -1.32$ V. The high oxidation potential is in accord with the Ru^{IV} oxidation state. The sharp NMR signals and the absence of an EPR signal indicate a singlet ground state. The d^4 electron system of the Ru^{IV} warrants the splitting of the π–d levels that is consistent with the UV–Vis spectrum of the complex exhibiting multiple MLCT bands [4].

The pyridyl or thiazolyl donor appended to NP at 2-position forms a planar five-member chelate ring with the Ru–Ru bond intact as illustrated in Scheme 1 [2]. The 2-hydroxyphenyl appendage, in contrast, lead to the scission of the Ru–Ru bond and provide mononuclear *cis*-[Ru(hpNP)$_2$(CO)$_2$][BF$_4$] (**3**). Recent work of Miyasaka et al. have shown that the ligands *N*-(2-pyridyl)-2-oxy-5-R-benzylaminate (R-salpy) form a family of diruthenium species [Ru$_2$(O$_2$CCH$_3$)$_2$(R-salpy)$_2$]$^-$ [5]. The flexible R-salpy ligands bind the diruthenium unit in the bridging/axial mode as shown in Scheme 4a. It is our assertion that the rigid hpNP does not allow the similar binding presumably due to steric strain associated with the six-member chelate ring (Scheme 4b).

Unlike the previous case, the scission of the Ru–Ru bond does not accompanied by the oxidation of the metal ion. The EPR signal ($g = 2.17$) confirms the oxidation state of the metal ion as Ru^I. The CO ligands are intact stabilizing the low oxidation state of the Ru. Use of the deprotonated hpNP ligand with [Ru$_2$(CO)$_4$(MeCN)$_6$][BF$_4$]$_2$ led to an intractable solid that was not characterized. Complex **3** undergoes three successive one-electron oxidations at $E_{p,a} = 0.76$, 1.07 and 1.34 V (Fig. 1). The electron transfer processes are irreversible and the couples involved are Ru^I/Ru^{II}, Ru^{II}/Ru^{III} and Ru^{III}/Ru^{IV}. The reduction profile of complex **3** involves two quasi-reversible ligand based waves at $E_{1/2}$ values at $-1.10(92)$ and at $-1.41(128)$ V.

The reaction of PPh$_3$ with [Ru$_2$(CO)$_4$(MeCN)$_6$][BF$_4$]$_2$ forms an adduct [Ru$_2$(CO)$_4$(MeCN)$_4$(PPh$_3$)$_2$][BF$_4$]$_2$ with the phosphine ligands coordinated at axial positions [6]. The diphosphine ligand dppm leads to oxidative cleavage of the Ru–Ru single bond. Each of the metal ion undergoes one-electron oxidation leading to the chloro bridged dimeric complex [Ru(μ-Cl)(dppm)(CO)(MeCN)]$_2$[BF$_4$]$_2$(**4**). The source of the Cl$^-$ is undoubtedly the CH$_2$Cl$_2$.
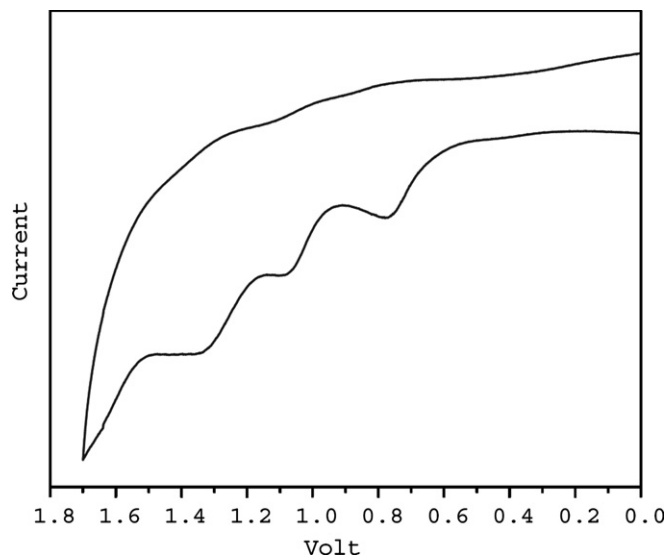

Fig. 1. Cyclic voltammogram for complex **3** in acetonitrile at a scan rate of 100 mV/s.

The ^{1}H NMR spectrum of diamagnetic complex **4** exhibits a singlet at 1.98 ppm for the coordinated CH$_3$CN. The methylene protons of dppm appear as a singlet at 5.27 ppm. A complex multiplet is observed in the aromatic region in the range 7.96–6.97 ppm corresponding to the phenyl protons of dppm. The ^{31}P{^{1}H} NMR spectrum of **4** exhibits two doublets at -2.90 ($^2J_{P–P} = 116.0$ Hz) and -11.65 ($^2J_{P–P} = 123.8$ Hz) ppm (Fig. 2). The chemical shift values resemble the four-member chelate ring formed by dppm with Ru metal center [7] and it supports the solid state structure obtained from X-ray crystallography.

2.2. Solid-state structures

The molecular structure of *cis*-[Ru$_2$(^{i}PrNP)$_2$(CO)$_4$-(OTf)$_2$] (**1**) as determined from X-ray diffraction study is shown in Fig. 3. Relevant bond distances and angles are tabulated in Table 1. The molecular structure of **1** consists

Scheme 4.
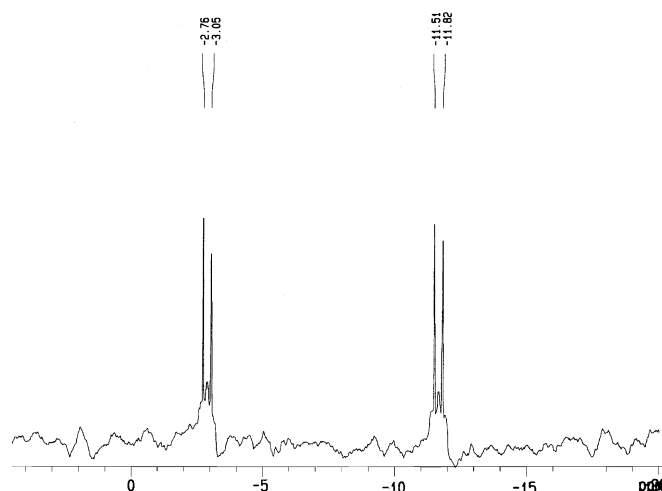
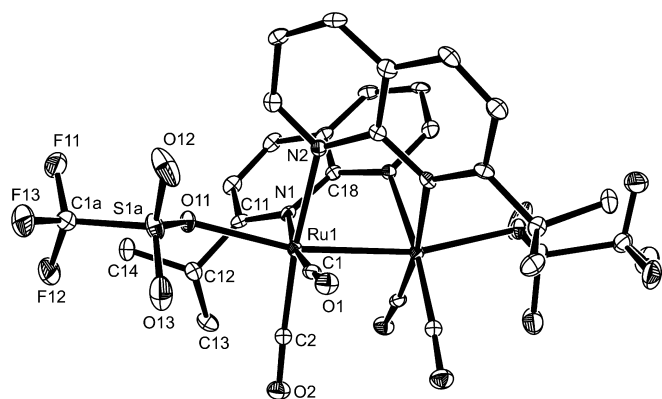Fig. 2. ^{31}P{^{1}H}NMR spectrum of the complex **4** in CD$_3$CN.

Fig. 3. ORTEP diagram of the *cis*-[Ru₂(*i*PrNP)₂(CO)₄(OTf)₂] (1) with important atoms labeled. Hydrogen atoms are omitted for the sake of clarity.

Table 1
Selected bond distances (Å) and bond angles (°) for 1

Ru1–Ru1	2.5969(4)	Ru1–O11	2.268(2)
Ru1–N1	2.213(3)	Ru1–C1	1.848(3)
Ru1–N2	2.170(3)	Ru1–C2	1.864(3)
N1–Ru1–N2	85.88(9)	Ru1–Ru1–O11	166.21(6)
N1–Ru1–C1	171.12(12)	C1–Ru1–C2	89.00(14)
N1–Ru1–C2	97.69(11)	O11–Ru1–N1	87.46(9)
N2–Ru1–C1	86.94(12)	O11–Ru1–N2	87.47(9)
N2–Ru1–C2	173.65(12)	O11–Ru1–C1	97.43(12)
Ru1–Ru1–N1	83.16(7)	O11–Ru1–C2	97.90(12)
Ru1–Ru1–N2	81.80(7)	Ru1–C1–O1	175.3(3)
Ru1–Ru1–C1	90.65(10)	Ru1–C2–O2	176.7(3)
Ru1–Ru1–C2	93.37(10)		

of a diruthenium unit with two *cis* *i*PrNP ligands bridging metal centers. Each ruthenium ion is bonded to two *cis* CO ligands and the axial sites are occupied by weakly coordinated triflate anions. The Ru–Ru bond distance is 2.5969(4) Å.

The X-ray structure of complex 2 consists of a tetracationic unit *trans*-[Ru(*t*BuNP)₂(MeCN)₂]⁴⁺ and the counter anions consist of two BF_4^- and one [NC(Me)C(Me)N]²⁻. The ORTEP plot of the cationic unit *trans*-[Ru(*t*BuNP)₂-(MeCN)₂]⁴⁺ is shown in Fig. 4 and the important bond distances and angles are provided in Table 2. The cationic part consists of a Ru atom in a pseudo octahedral environment coordinated to two *t*BuNP ligands in bidentate chelate modes and two *trans* CH₃CN bound axially. The *trans*-[Ru(*t*BuNP)₂(MeCN)₂]⁴⁺ has an crystallographically imposed center of inversion at Ru. Although the NP ligands are widely known to bridge dimetal units, bidentate chelate mode is observed in complex 2 with very acute N–Ru–N angle of 62.97(19)°. The Ru–N(NP) distances are 2.104(5) and 2.136(5) Å and Ru–N(CH₃CN) distance is 2.018 Å. The short Ru–N(axial) distances are the manifestation of the high oxidation state Ru^{IV} as opposed to the Ru^{II}.

The most notable observation in the X-ray structure of the complex is the planar dianion *anti*-[NC(Me)-
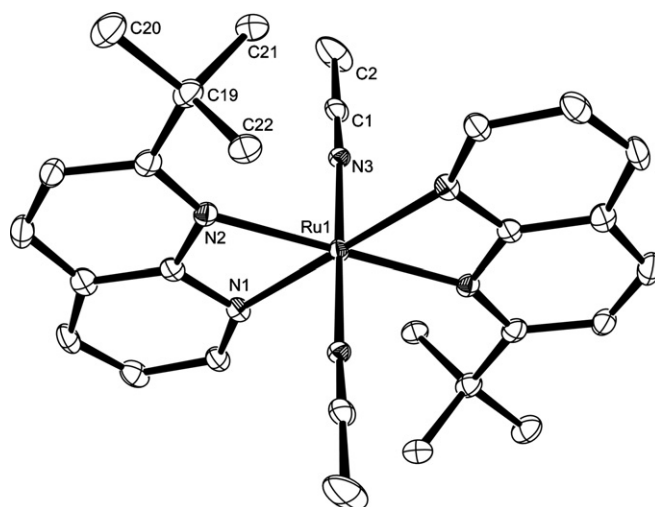

Fig. 4. ORTEP diagram of the cationic unit *trans*-[Ru(*t*BuNP)₂-(MeCN)₂]²⁺ in compound 2 with important atoms labeled. Hydrogen atoms are omitted for the sake of clarity.

Table 2
Selected bond distances (Å) and bond angles (°) for 2

Ru1–N1	2.104(5)	Ru1–N3	2.018(5)
Ru1–N2	2.136(5)		
N1–Ru1–N2	62.97(19)	N1–Ru1–N3′	90.85(18)
N1–Ru1–N3	89.15(18)	N2–Ru1–N3	90.05(19)
N1–Ru1–N2′	117.03(19)	N1′–Ru1–N2	117.03(19)

C(Me)N]²⁻. The ORTEP plot with C=N and C—C distances are shown in Fig. 5. A search at the CSD reveals no structural precedent for this species. However, identical species has been reported to bridge two W^{II} centers in [{HB-(Me₂pz)₃}W(CO)₂]₂{μ-NC(Me)C(Me)N} (HB(Me₂pz)₃⁻ = (3, 5-dimethyl pyrazol-1-yl)borate anion) [8]. Comparison of the metrical parameters reveals that the C–N distance (1.28(3) Å) in the ditungsten complex is longer
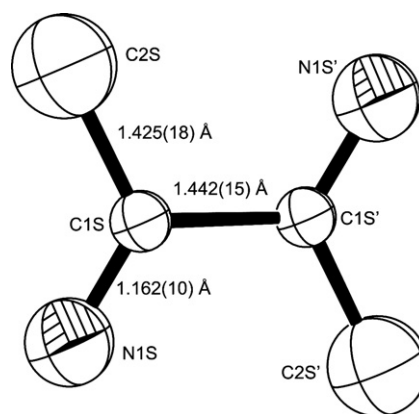

Fig. 5. ORTEP diagram of the dianion *anti*-[NC(Me)C(Me)N]²⁻ in compound 2 with the atoms labeled. The bond lengths are shown in figure. Hydrogen atoms are omitted for the sake of clarity. Thermal ellipsoids are drawn to 30% probability.

and the C–C distance (1.40(4) Å) is shorter than the corresponding distances observed for the free dianion in complex **2**. The *anti*-[NC(Me)C(Me)N]$^{2-}$ in **2** is essentially planar with N1S–C1S–C1S′–N1S′ torsion angle 180.0(10)°. The non-planarity and the lengthening of the C–N distances of the bridging dianion in [{HB(Me$_2$pz)$_3$}-W(CO)$_2$]$_2${μ-NC(Me)C(Me)N} are presumably due to coordination to the metal ions.

The cationic unit *cis*-[Ru(hpNP)$_2$(CO)$_2$]$^+$ in complex **3** consists of a Ru atom bonded to two hpNP ligands and two *cis* CO ligands. The ORTEP plot of the cationic unit *cis*-[Ru(hpNP)$_2$(CO)$_2$]$^+$ is shown in Fig. 6 and important bond distances and bond angles are tabulated in Table 3. The Ru atom forms a non-planar Ru–N–(C)$_3$–O six-member chelate ring. Two independent molecules were located in the asymmetric unit with slight differences in metrical parameters. The Ru–N distances are in the range of 2.085(4)–2.098(4) Å. The O–Ru–N angles of the Ru–N–
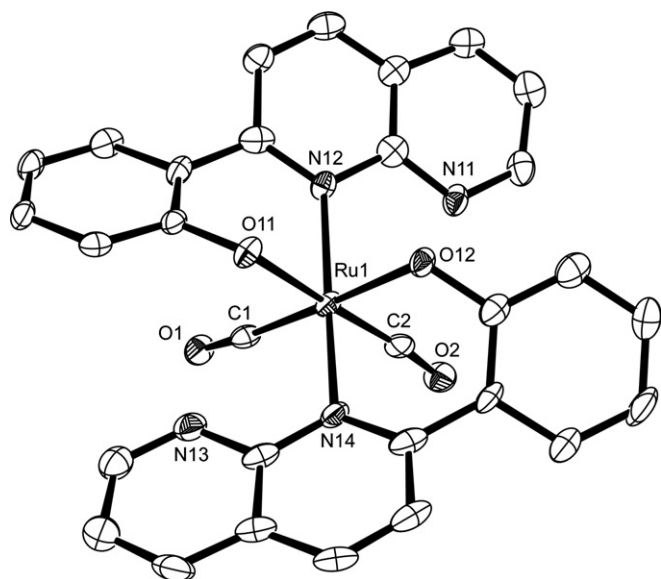
(C)$_3$–O chelate ring are in the range of 82.42(19)–83.19(19)°.

The cationic unit [{Ru(μ-Cl)(dppm)(CO)(MeCN)}$_2$]$^{2+}$ in complex **4** consists of a diruthenium ESBO structure held by two Cl bridges. The ORTEP plot of the cationic unit [{Ru(μ-Cl)(dppm)(CO)(MeCN)}$_2$]$^{2+}$ is shown in Fig. 7 and important bond distances and angles are tabulated in Table 4. The molecule has an inversion center located at mid of the Ru–Ru vector. Each Ru^{II} metal center is in a pseudo-octahedral environment coordinated to two phosphorous of dppm forming a four member Ru–P–C–P chelate ring, one MeCN and one CO which are *trans* position to each other and two bridging chlorides. The bond order between two Ru centers are zero corresponding to electron configuration $\sigma^2\pi^2\delta^2\delta^{*2}\pi^{*2}\sigma^{*2}$. The Ru–Cl bond distances are 2.4883(12) and 2.4895(12) Å. The Ru–Cl–Ru, Cl–Ru–Cl and P–Ru–P angles are 94.74(4)°, 85.26(4)° and 72.03(4)° respectively.
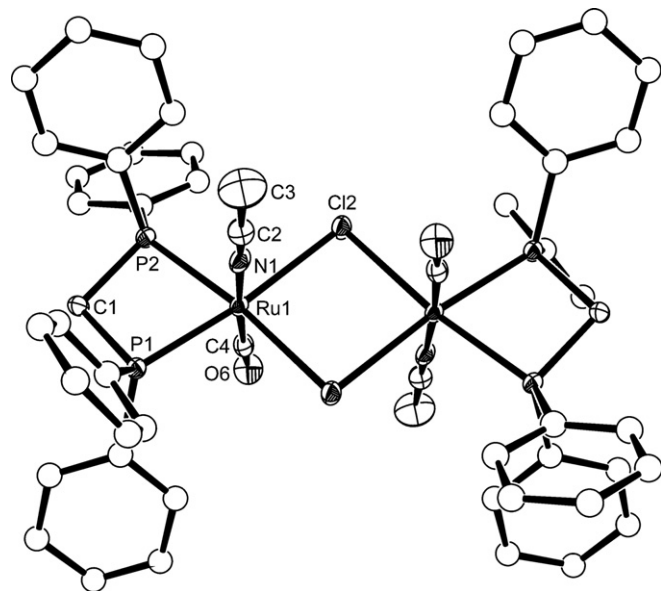

Fig. 6. ORTEP diagram of the cationic unit *cis*-[Ru(hpNP)$_2$(CO)$_2$]$^+$ in compound **3** with important atoms labeled. Hydrogen atoms are omitted for the sake of clarity.

Fig. 7. ORTEP diagram of the cationic unit [Ru$_2$Cl$_2$(dppm)$_2$(CO)$_2$-(MeCN)$_2$]$^{2+}$ in compound **4** with important atoms labeled. Hydrogen atoms are omitted for the sake of clarity. Carbon atoms of the phenyl rings of the dppm ligand are shown as circles of arbitrary radius.

Table 3
Selected bond distances (Å) and bond angles (°) for **3**

Ru1–O11	2.089(5)	Ru1–C1	1.871(7)
Ru1–O12	2.098(5)	Ru1–C2	1.867(8)
Ru1–N12	2.125(5)	C1–O1	1.132(9)
Ru1–N14	2.125(6)	C2–O2	1.141(9)
O11–Ru1–O12	82.24(18)	N12–Ru1–C1	91.4(3)
O11–Ru1–N12	82.42(19)	N12–Ru1–C2	97.8(3)
O11–Ru1–N14	87.63(19)	N14–Ru1–C1	97.5(3)
O11–Ru1–C1	94.6(3)	N14–Ru1–C2	91.8(3)
O11–Ru1–C2	177.1(3)	C1–Ru1–C2	88.3(3)
O12–Ru1–N12	88.09(19)	Ru1–O11–C24	116.1(4)
O12–Ru1–N14	82.46(19)	Ru1–O12–C44	115.7(4)
O12–Ru1–C1	176.9(3)	Ru1–C1–O1	174.0(7)
O12–Ru1–C2	94.9(3)	Ru1–C2–O2	173.5(7)
N12–Ru1–N14	167.13(19)		

Table 4
Selected bond distances (Å) and bond angles (°) for **4**

| Ru1–Cl2	2.4895(12)	Ru1–N1	2.082(4)
Ru1–P1	2.2788(13)	Ru1–C4	1.883(5)
Ru1–P2	2.2868(13)	Ru1–Cl2′	2.4883(12)
Cl2–Ru1–P1	173.89(4)	Cl2′–Ru1–P1	100.13(4)
Cl2–Ru1–P2	102.49(4)	P2–Ru1–N1	92.01(11)
Cl2–Ru1–N1	85.85(11)	P2–Ru1–C4	90.88(14)
Cl2–Ru1–C4	92.31(13)	Cl2′–Ru1–P2	171.95(4)
Cl2–Ru1–Cl2′	85.26(4)	N1–Ru1–C4	176.85(17)
P1–Ru1–P2	72.03(4)	Cl2′–Ru1–N1	86.31(11)
P1–Ru1–N1	91.59(11)	Cl2′–Ru1–C4	90.99(13)
P1–Ru1–C4	90.49(13)	Ru1–Cl2–Ru1′	94.74(4)
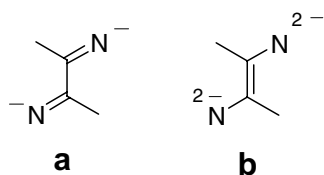
Scheme 5.

2.3. The chemical consequence

One of the themes of the organometallic chemistry is to synthesize new chemical species through C–C bond formation and to stabilize the highly reactive or unstable ligands by metal centers. The neutral anti-butane-2,3-diimine is highly unstable and has never been isolated. We find a report where the dianion anti-$[NC(Me)C(Me)N]^{2-}$ (Scheme 5a) is generated from the reductive coupling of acetonitrile and it bridges two W^{II} ions which is structurally characterized [8]. Infrared (IR) multiphoton dissociation spectroscopy of the cationic niobium–acetonitrile complex revealed the metallacyclic species $[Nb^{III}(MeCN)_3\{NC(Me)C(Me)N\}]^+$ which is formed by the intramolecular reductive nitrile coupling reaction [9]. In addition to the dianion, there is also a possibility of the (E)-butene-2,3-diimido tetraanionic ligand from the four-electron reduction of acetonitriles (Scheme 5b) [10]. The possibility of

the tetraanion in this work was ruled out from the structural parameters.

We believe that the dianion anti-$[NC(Me)C(Me)N]^{2-}$ in complex 2 is generated from the reductive coupling of two acetonitrile molecules as in the cases reported earlier. The reactions involve are complex and we offer a tentative mechanism in Scheme 6 based on the products formation. The Ru–Ru single bond undergoes homolytic cleavage yielding metal based free radical. The $Ru^{I\cdot}$ is oxidized to Ru^{III} producing two iminyl radicals that undergo coupling reaction to produce L^{2-}. The $[Ru(^tBuNP)_2(MeCN)_2]^{3+}$ undergoes a further oxidation to 16-electron Ru^{IV} complex 2. The 18-electron $[Ru(CO)_3(MeCN)_2]$ is formed as a by-product of this reaction which is confirmed by IR spectra [11].

The net reaction involves the use of one equivalent of ^tBuNP for each Ru and no additional CH_3CN is needed. It accounts for the less than 50% isolated yield of 2 calculated based on Ru and explains the isolation of the identical products in dichloromethane albeit in low yield.

The reaction of $[Ru_2(CO)_4(MeCN)_6][BF_4]_2$ with dppm in dicholoromethane is rather straightforward in comparison. The bulky phosphine leads to hemolytic cleavage of Ru–Ru single bond generating $Ru^{I\cdot}$ that donate the electron to C–Cl σ^* orbital of the CH_2Cl_2 allowing the production of Cl^- and the final compound is the chloro bridged Ru(II) product. The Ru–Ru bond scission by the hpNP is not accompanied by the oxidation of Ru.
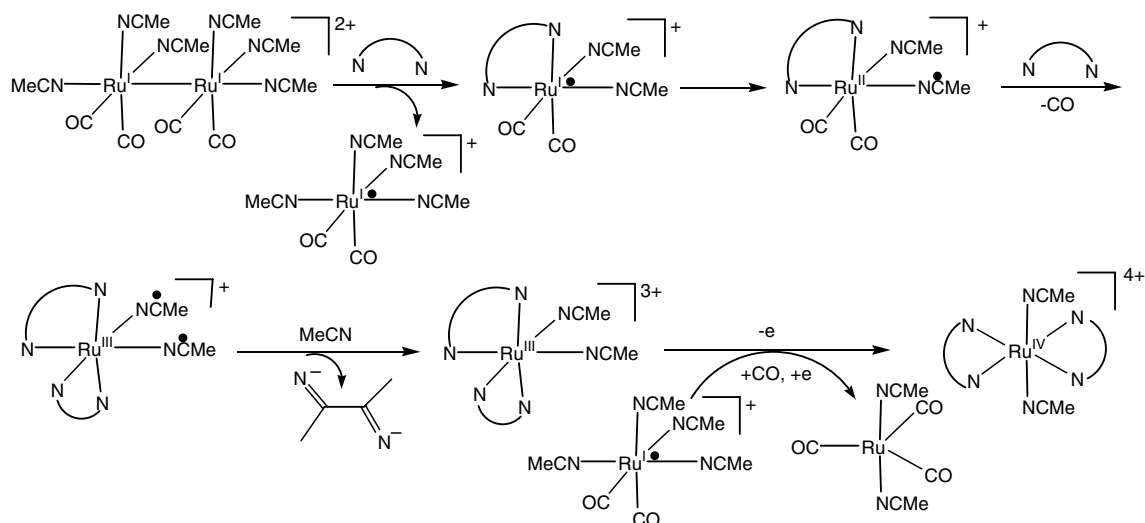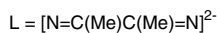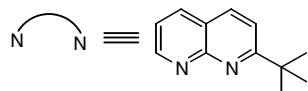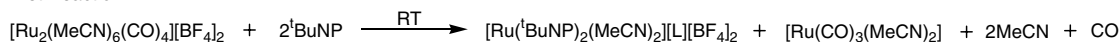
Scheme 6.

3. Summary

The isopropyl groups are placed at sites trans to the Ru–Ru bond in $[Ru_2(CO)_4(MeCN)_6]^{2+}$ utilizing the NP based ligand ^iPrNP. The isolated product is the cis-$[Ru_2(^iPrNP)_2$-$(CO)_4(OTf)_2]$ with the Ru–Ru single bond being intact. On the contrary, the use of ^tBuNP, hpNP and dppm result in the cleavage of the Ru–Ru single bond resulting in the mononuclear Ru complexes. The reaction of $[Ru_2(CO)_4$-$(MeCN)_6][BF_4]_2$ with ^tBuNP leads the formation of the dianion of anti-butane-2,3-diimine through reductive acetonitrile coupling. Although the free *anti*-butane-2,3-diimine is unstable and never been isolated, the corresponding dianion is stabilized as the counter anion of the cation *trans*-$[Ru(^tBuNP)_2(MeCN)_2]^{4+}$ in complex **2** which is structurally characterized. The sterically demanding hpNP ligand forms the Ru^I mononuclear complex cis-$[Ru(hpNP)_2(CO)_2][BF_4]$ (**3**) through non-oxidative cleavage of Ru–Ru single bond whereas dppm ligand provides the dimeric ESBO complex $[\{Ru(\mu\text{-}Cl)(dppm)(CO)(MeCN)\}_2][BF_4]_2$ (**4**) via oxidative cleavage of Ru–Ru bond in dichloromethane.

4. Experimental

4.1. Materials

All manipulations were carried out under an inert atmosphere with the use of standard Schlenk-line techniques. Glasswares were flame-dried under vacuum prior to use. Solvents were dried by conventional methods [12], distilled over nitrogen and deoxygenated prior to use. $RuCl_3 \cdot nH_2O$ (39% Ru) was purchased from Arora Matthey, India. Compound $[Ru_2(CO)_4(CH_3CN)_6][BF_4]_2$ was synthesized following a procedure similar to the synthesis of $[Ru_2(CO)_4(CH_3CN)_6][PF_6]_2$ [6]. The ligands ^iPrNP, ^tBuNP and hpNP were prepared by the Friedlander condensation of 2-aminonicotinaldehyde with corresponding acyl derivatives [13]. The reagent dppm was purchased from Aldrich and used without further purification.

4.2. Physical measurements

Infrared spectra were recorded in the range 4000–400 cm^{-1} on a Vertex 70 Bruker spectrophotometer on KBr pellets. ^1H NMR and $^{31}P\{^1H\}$ NMR spectra were obtained on a JEOL JNM-LA 400 MHz spectrometer. ^1H NMR chemical shifts were referenced to the residual hydrogen signal of the deuterated solvents and ^{31}P NMR chemical shifts were referenced to an external 85% solution of phosphoric acid in D_2O. Electronic absorptions were measured on a Lambda-20 Perkin–Elmer spectrophotometer. EPR spectra were recorded on a Bruker EMX X-band spectrometer. Cyclic voltammetric studies were performed on a BAS Epsilon electrochemical workstation in acetonitrile with 0.1 M tetra-*n*-Butylammonium hexafluorophosphate (TBAPF$_6$) as the supporting electrolyte. The working electrode was a BAS Pt disk electrode, the refer-ence electrode was Ag/AgCl and the auxiliary electrode was a Pt wire. The ferrocene/ferrocenium couple occurs at $E_{1/2} = +0.51$ (77) V versus Ag/AgCl under the same experimental conditions.

4.3. Synthesis

4.3.1. Synthesis of cis-[Ru$_2$(^{i}PrNP)$_2$(CO)$_4$(OTf)$_2$] (1)

An acetonitrile solution (10 mL) of 2-^{i}PrNP (17 mg, 0.098 mmol) was added drop-wise to an acetonitrile solution (10 mL) of $[Ru_2(CO)_4(MeCN)_6][BF_4]_2$ (34 mg, 0.046 mmol) and the solution was stirred for 8 h at room temperature. The resulting yellow colored solution was concentrated under vacuum, and 15 mL of diethyl ether was added with stirring to induce precipitation. The solid residue obtained was washed with ether (3×5 mL) and dried in vacuum. The crystallized cis-$[Ru_2(^iPrNP)_2$-$(CO)_4(OTf)_2]$ (**1**) was obtained by layering pet ether onto the acetone solution of cis-$[Ru_2(^iPrNP)_2(CO)_4][BF_4]_2$ and [*n*-Bu$_4$N][OTf]. Yield: 0.041 g (85%). ^1H NMR (CD$_3$CN, δ): 8.67 (d, 2H), 8.43 (d, 2H), 8.03 (d, 2H), 8.01 (m, 2H), 7.20 (m, 2H), 4.35 (m, 2H), 1.71 (d, 6H), 1.47 (d, 6H). IR (KBr) data (cm^{-1}): v (CO): 2045, 1963; v (OTf$^-$): 1260. UV–Vis spectrum [λ_{max}, nm (ε, dm^3 mol^{-1} cm^{-1})] (in CH$_3$CN): 273 (sh), 302 (3.35×10^3), 367 (2.02×10^3).

4.3.2. Synthesis of trans-[Ru(^{t}BuNP)$_2$(MeCN)$_2$][BF$_4$]$_2$-[NC(Me)C(Me)N] (2)

An acetonitrile solution (10 mL) of ^tBuNP (24 mg, 0.134 mmol) was added drop-wise to an acetonitrile solution (15 mL) of $[Ru_2(CO)_4(CH_3CN)_6][BF_4]_2$ (45 mg, 0.061 mmol) and the solution was stirred for 8 h at room temperature. The resulting yellow colored solution was concentrated under vacuum, and 15 mL of diethyl ether was added with stirring to induce precipitation. It was recrystallized by layering diethyl ether onto the acetonitrile solution of the compound. Yield: 40 mg (40% based on Ru). ^1H NMR (CD$_3$CN, δ): 9.37 (d, 2H), 8.60 (m, 4H), 7.85 (d, 2H), 7.80 (q, 2H), 2.20 (s, 6H), 2.07 (s, 6H), 1.70 (s, 18H). IR (KBr) data (cm^{-1}): $v(BF_4^-)$: 1057. UV–Vis spectrum [λ_{max}, nm (ε, dm^3 mol^{-1} cm^{-1})] (in CH$_3$CN): 264 (6.08×10^3), 278 (sh), 311 (3.37×10^3), 382 (2.03×10^3), 465 (1.15×10^3).

4.3.3. Synthesis of cis-[Ru(hpNP)$_2$(CO)$_2$][BF$_4$] (3)

An acetonitrile solution of hpNP (22 mg, 0.098 mmol) was added drop-wise to an acetonitrile solution of $[Ru_2(CO)_4(MeCN)_6][BF_4]_2$ (35 mg, 0.047 mmol). There was an immediate color change to red from yellow and the solution was stirred for 8 h. The resulting solution was concentrated under vacuum and 15 mL of benzene was added with stirring to induce precipitation. The solid residue obtained was washed with benzene (3×5 mL) and dried in vacuum. Yield: 24 mg (72%). IR (KBr) data (cm^{-1}): $v(CO)$: 2036, 1954; $v(BF_4^-)$: 1074. UV–Vis spectrum [λ_{max}, nm (ε, dm^3 mol^{-1} cm^{-1})] (in CH$_3$CN): 253 (2.18×10^4), 321 (1.55×10^4), 461 (3.28×10^3).

4.3.4. Synthesis of [Ru(μ-Cl)(dppm)(CO)(CH₃CN)]₂-[BF₄]₂ (4)

An dichloromethane solution (10 mL) of dppm (27 mg, 0.070 mmol) was added drop-wise to a dichloromethane solution (15 mL) of $[Ru_2(CO)_4(MeCN)_6][BF_4]_2$ (25 mg, 0.034 mmol) and the solution was stirred for 8 h at room temperature. The resulting light-yellow turbid solution was concentrated under vacuum, and 15 mL of ether was added with stirring to induce precipitation. The yellow residue obtained was washed with ether (3 × 5 mL) and dried in vacuum. Yield: 32 mg (70%). ^1H NMR (CD₃CN, δ): 7.96–6.97 (m, 40H), 5.27 (s, 4H), 1.98 (s, 6H). $^{31}P\{^1H\}$ NMR (CD₃CN, δ): −2.90 (d, $J_{P–P}$ = 116.0 Hz), −11.65 (d, $J_{P–P}$ = 123.8 Hz). IR (KBr) data (cm⁻¹): v(CO): 2045, 1970; $v(BF_4^-)$ 1060. UV–Vis spectrum [λ_{max}, nm (ε, dm³ mol⁻¹ cm⁻¹)] (in CH₃CN): 220 (2.11 × 10³), 303 (9.28 × 10²), 316 (sh).

4.4. X-ray data collection and refinement

Single-crystal X-ray studies were performed on a CCD Bruker SMART APEX diffractometer equipped with an Oxford Instruments low-temperature attachment. Data were collected at 100(2) K using graphite-monochromated Mo Kα radiation (λ_α = 0.71073 Å). The frames were indexed, integrated and scaled using SMART and SAINT software package, data were corrected for absorption using the SADABS program and the structures were solved and refined using SHELX suite of programs [14]. Hydrogen atoms of the ligands, unless mentioned otherwise, were included in the final stages of the refinement and were refined with a typi-

cal riding model. ORTEP-III was used to produce the diagrams with the thermal ellipsoids drawn at 50% probability [15] unless mentioned otherwise. Pertinent crystallographic data for compounds **1**–**4** are summarized in Table 5.

X-ray quality crystals of cis-[Ru₂(^{i}PrNP)₂(CO)₄(OTf)₂] (**1**) were harvested by layering petroleum ether onto the acetone solution of cis-[Ru₂(^{i}PrNP)₂(CO)₄][BF₄]₂ and [n-Bu₄N][OTf] in a 8 mm O.D. sealed glass tube. X-ray quality crystals of $trans$-[Ru(^{t}BuNP)₂(MeCN)₂][BF₄]₂-[NC(Me)C(Me)N] (**2**) were obtained by layering diethyl ether onto the acetonitrile solution of **2** in a 8 mm OD sealed glass tube. Only half of molecule **2** resides in the asymmetric unit. The tetrafluoroborate anion was found to be disordered and modeled satisfactorily. All non-hydrogen atoms except the B and F atoms of the tetrafluoroborate anions were refined with anisotropic thermal parameters. X-ray quality crystals of cis-[Ru(hpNP)₂-(CO)₂][BF₄] (**3**)CH₃COCH₃ were obtained by layering petroleum ether onto the acetone solution of **3**. In the asymmetric unit, two independent molecules of **3** were located. One of the solvate acetone molecules was found to be disordered and restrains were applied. All non-hydrogen atoms except carbon and O atoms of two acetone solvent molecules were refined with anisotropic thermal parameters. The phenolic H atom was not assigned in the structure. X-ray quality crystals of [Ru(μ-Cl)(dppm)(CO)-(MeCN)]₂[BF₄]₂ (**4**)CH₂Cl₂ were obtained by layering pet ether onto the dichloromethane solution of **4**. In the asymmetric unit, only half of molecule **4** resides. All non-hydrogen atoms were refined with anisotropic thermal parameters.

Table 5
Crystallographic data and refinement parameters for **1**, **2**, **3** · CH₃COCH₃ and **4** · CH₂Cl₂

	1	2	3 · CH₃COCH₃	4 · CH₂Cl₂
Empirical formula	C₂₈H₂₄F₆N₄O₁₀Ru₂S₂	C₃₂H₄₀N₈B₂F₈Ru	C₃₃H₂₁N₄O₅BF₄Ru	C₅₈H₅₄Cl₆N₂O₂P₄B₂F₈Ru₂
Formula weight	956.79	811.41	741.42	1523.37
Crystal system	Monoclinic	Monoclinic	Monoclinic	Monoclinic
Space group	C2/c	P2₁/c	P2₁/c	P2₁/n
a (Å)	21.812(2)	9.063(5)	14.2298(10)	12.1882(10)
b (Å)	8.4070(8)	17.044(5)	16.3101(11)	13.3343(11)
c (Å)	17.6142(17)	11.591(5)	28.2172(17)	20.1327(16)
α (°)				
β (°)	91.573(3)	108.217(5)	112.942(3)	106.0720(10)
γ (°)				
V (Å³)	3228.8(5)	1700.7(13)	6030.9(7)	3144.1(4)
Z	4	2	4	2
ρ_{calcd} (g cm⁻³)	1.968	1.584	1.633	1.609
μ (mm⁻¹)	1.164	0.543	0.595	0.904
$F(000)$	1896	828	2976	1528
Reflections collected	10418	9780	30520	18042
Unique	3941	3455	10267	6393
Observed [$I > 2\sigma(I)$]	3035	2801	7330	5266
Number of variables	232	221	836	380
Goodness-of-fit	1.03	1.14	1.05	1.11
Final R indices [$I > 2\sigma(I)$][a]	R_1 = 0.0371	R_1 = 0.0620	R_1 = 0.0683	R_1 = 0.0607
	wR_2 = 0.0781	wR_2 = 0.1446	wR_2 = 0.1426	wR_2 = 0.1348

[a] $R_1 = \sum \|F_o| - |F_c\| / \sum |F_o|$ with $F_o^2 > 2\sigma(F_o^2)$. $wR_2 = [\sum w(|F_o^2| - |F_c^2|)^2 / \sum |F_o^2|^2]^{1/2}$.

5. Supporting information

Crystallographic data for the structural analysis for the complexes **1**–**4** have been deposited with the Cambridge Crystallographic Data Centre, CCDC Nos. 607517–607520 respectively. Copies of this information may be obtained free of charge from the Director, CCDC, 12 Union Road, Cambridge CB2 1EZ, UK (fax: +44 1223 336 033, or e-mail: deposit@ccdc.cam.ac.uk).

Acknowledgments

References

[1] (a) C.S. Campos-Fernandez, L.M. Thomson, J.R. Galan-Mascaros, X. Ouyang, K.R. Dunbar, Inorg. Chem. 41 (2002) 1523;
(b) J.-P. Collin, A. Jouaiti, J.-P. Sauvage, W.C. Kaska, M.A. McLoughlin, N.L. Keder, W.T.A. Harrison, G.D. Stucky, Inorg. Chem. 29 (1990) 2238;
(c) E. Binamira-Soriaga, N.L. Keder, W.C. Kaska, Inorg. Chem. 29 (1990) 3167;
(d) R.P. Thummel, Y. Decloitre, Inorg. Chim. Acta 128 (1987) 245;
(e) R.P. Thummel, F. Lefoulon, D. Williamson, M. Chavan, Inorg. Chem. 25 (1986) 1675;
(f) E. Binamira-Soriaga, S.D. Sprouse, R.J. Watts, W.C. Kaska, Inorg. Chim. Acta. 84 (1984) 135;
(g) W.R. Tikkanen, C. Krüger, K.D. Bomben, W.L. Jolly, W.C. Kaska, P.C. Ford, Inorg. Chem. 23 (1984) 3633;
(h) A.T. Baker, W.R. Tikkanen, W.C. Kaska, P.C. Ford, Inorg. Chem. 23 (1984) 3254;
(i) W. Tikkanen, E. Binamira-Soriaga, W. Kaska, P.C. Ford, . Inorg. Chem. 23 (1984) 141.
[2] S.K. Patra, N. Sadhukhan, J.K. Bera, Inorg. Chem. 45 (2006) 4007.
[3] S.K. Patra, J.K. Bera, unpublished result. Crystal data for *cis*-[Ru$_2$(MeNP)$_2$(CO)$_4$(OTf)$_2$]: formula C$_{24}$H$_{16}$F$_6$N$_4$O$_{10}$Ru$_2$S$_2$, orthorhombic, space group *Pbca*, $a = 13.301(15)$ Å, $b = 14.195(5)$ Å, $c = 33.346(5)$ Å, $V = 6296.0(3)$ Å^3, $R_1 = 0.0543$, $wR_2 = 0.1212$. Ru1–Ru2 = 2.5994(9) Å.
[4] (a) J.F. Wishart, A. Bino, H. Taube, Inorg. Chem. 25 (1986) 3318;
(b) C. Creutz, H. Taube, J. Am. Chem. Soc. 95 (1973) 1086.
[5] (a) H. Miyasaka, T. Izawa, K. Sugiura, M. Yamashita, Inorg. Chem. 42 (2003) 7683;
(b) H. Miyasaka, C. Kachi-Terajima, T. Ishii, M. Yamashita, J. Chem. Soc., Dalton Trans. (2001) 1929.
[6] W.J. Klemperer, B. Zhong, Inorg. Chem. 32 (1993) 5821.
[7] P.E. Garrou, Chem Rev. 81 (1981) 229.
[8] C.G. Young, C.C. Philipp, P.S. White, J.L. Templeton, Inorg. Chem. 34 (1995) 6412.
[9] B.M. Reinhard, A. Lagutschenkov, J. Lemaire, P. Maitre, P. Boissel, G. Niedner-Schatteburg, J. Phys. Chem. A 108 (2004) 3350.
[10] (a) For the planar (E)-butene-2,3-diimido tetraanionic ligand the C–N distances are in the range of 1.38(1)–1.40(1) Å and the C–C distance are in the range of 1.34(1)–1.35(1) Å P.A. Finn, M.S. King, P.A. Kilty, R.E. McCarley, J. Am. Chem. Soc. 97 (1975) 220;
(b) F.A. Cotton, W.T. Hall, Inorg. Chem. 17 (1978) 3525;
(c) F.A. Cotton, W.T. Hall, J. Am. Chem. Soc. 101 (1979) 5094;
(d) R. Duchateau, A.J. Williams, S. Gambarotta, M.Y. Chiang, Inorg. Chem. 30 (1991) 4863;
(e) D.G. Blight, R.L. Deutscher, D.L. Kepert, J. Chem. Soc., Dalton Trans. (1972) 87.
[11] The colorless [Ru(CO)$_3$(MeCN)$_2$] was isolated from the mother liquor during the crystallization of the compound *trans*-[Ru(^{t}BuNP)$_2$(MeCN)$_2$][BF$_4$]$_2$[NC(Me)C(Me)N] (**2**) in MeCN/Et$_2$O solvents and characterized by a single peak in IR spectra centered at 1983 cm^{-1} (using NaCl pellet) A.J. Edwards, N.E. Leadbeater, J. Lewis, P.R. Raithby, J. Organomet. Chem. 503 (1995) 15.
[12] D.D. Perrin, W.L.F. Armarego, D.R. Perrin, Purification of Laboratory Chemicals, second ed., Pergamon Press, New York, 1980.
[13] (a) K.V. Reddy, K. Mogilaiah, B. Sreenivasulu, J. Indian Chem. Soc. 63 (1986) 443;
(b) R.P. Thummel, F. Lefoulon, D. Cantu, R.J. Mahadevan, J. Org. Chem. 49 (1984) 2208;
(c) T.C. Majewicz, P. Caluwe, J. Org. Chem. 39 (1974) 720;
(d) E.M. Hawes, D.G. Wibberley, J. Chem. Soc. (1966) 315.
[14] (a) SAINT+ Software for CCD diffractometers; Bruker AXS, Madison,WI, 2000;
(b) G.M. Sheldrick, SADABS Program for Correction of Area Detector Data, University of Göttingen, Göttingen, Germany, 1999;
(c) SHELXTL Package v. 6.10, Bruker AXS, Madison, WI, 2000;
(d) SHELXS-86 and SHELXL-97, University of Göttingen: Göttingen, Germany, 1997.
[15] L.J. Farrugia, J. Appl. Cryst. 30 (1997) 565.